

# Mechanisms Controlling World Water Chemistry

**Abstract.** *On the basis of analytical chemical data for numerous rain, river, lake, and ocean samples, the three major mechanisms controlling world surface water chemistry can be defined as atmospheric precipitation, rock dominance, and the evaporation-crystallization process.*

Some of the mechanisms that control the chemical composition of the major dissolved salts of the waters of the earth have been discussed by Conway (1), Gorham (2), Mackenzie and Garrels (3), and Sillén (4). However, from further investigation I have observed that many aspects of the overall mechanisms are still poorly understood. For this reason and because of increased interest in recent years in the chemical composition of surface waters, the objective of this report is to elucidate the major natural mechanisms controlling world water chemistry.

The major cations that characterize the end-members of the world's sur-

face waters are Ca for freshwater bodies and Na for high-saline water bodies. Plotted in Fig. 1 is the weight ratio  $\text{Na}/(\text{Na} + \text{Ca})$  on the x-axis and the variation in total salinity on the y-axis. The compositions of the world's surface waters (5, 6) plot as two diagonal lines on Fig. 1. This ordered arrangement can serve as a basis for discussion of the several mechanisms that control world water chemistry.

The first of these mechanisms is atmospheric precipitation. The chemical compositions of low-salinity waters (Fig. 1) are controlled by the amount of dissolved salts furnished by precipitation. These waters consist mainly of

the tropical rivers of Africa and South America having sources in thoroughly leached areas of low relief in which the rate of supply of dissolved salts to the rivers is very low and the amount of rainfall is high—much greater in proportion to the low amount of dissolved salts supplied from the rocks. In addition, the composition of this precipitation differs from that of rock-derived dissolved salts. The data of Gibbs (5) for 16 tributaries of the Amazon River show that salts carried in rainfall rather than derived from rocks account for the major portion of the dissolved salts present in many of these tributary rivers. Gibbs's data (5) indicate also that, except for a few rock-derived elements such as Si and K in the tributary rivers, the compositions of the dissolved salts of many of the tropical tributaries of the Amazon River are similar to that of seawater. Many of these Amazon tributaries are thousands of kilometers

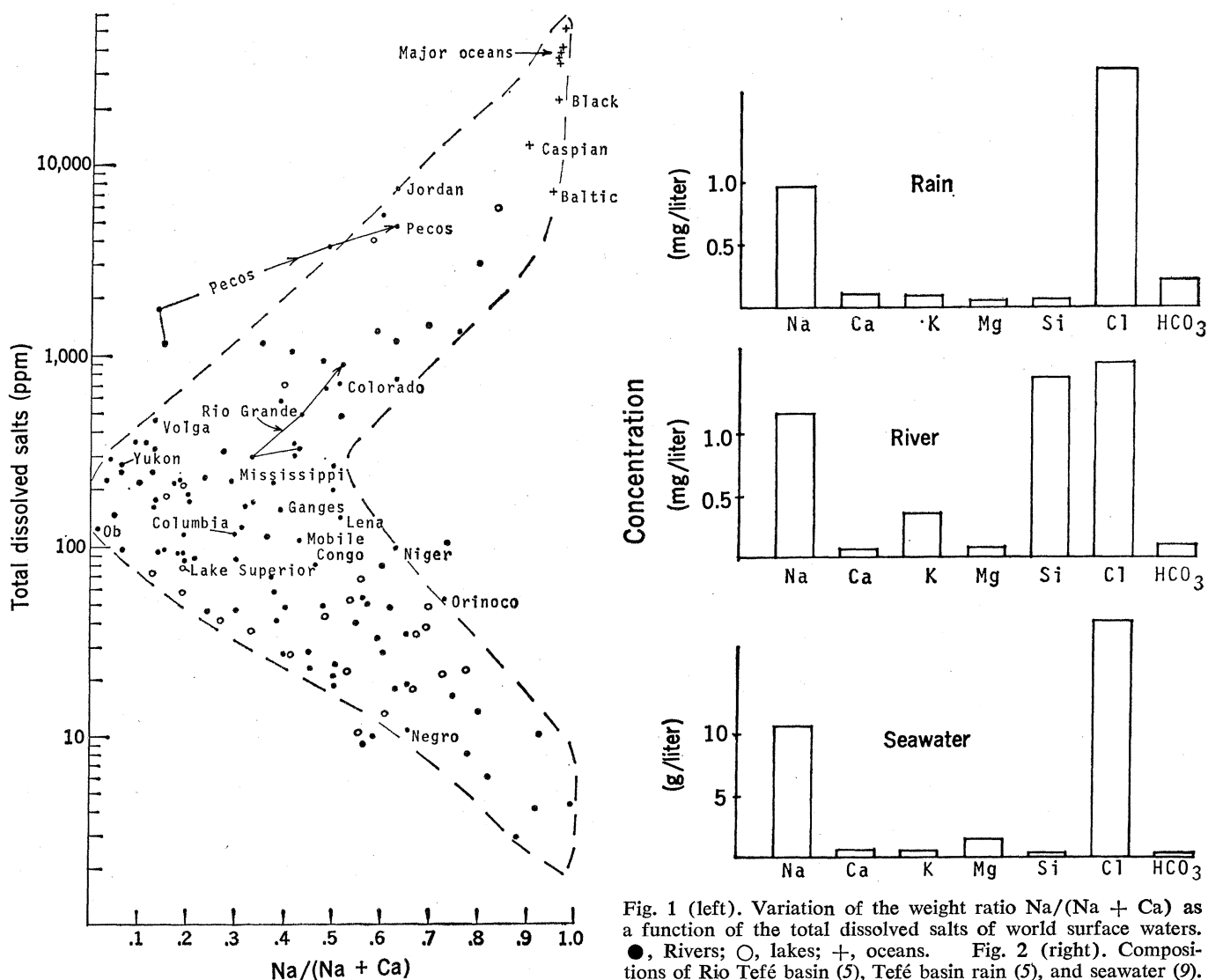


Fig. 1 (left). Variation of the weight ratio  $\text{Na}/(\text{Na} + \text{Ca})$  as a function of the total dissolved salts of world surface waters. ●, Rivers; ○, lakes; +, oceans. Fig. 2 (right). Compositions of Rio Tefé basin (5), Tefé basin rain (5), and seawater (9).

from the sea, an indication that the supply of dissolved salts to freshwater bodies by atmospheric precipitation is not limited to bodies of water near coasts (Fig. 1), as discussed by Gorham (2) for lakes near oceans.

A comparison of the composition of rainwater and river water of Rio Tefé (a low-relief Amazon tributary), as an example of a tropical river, with that of seawater (Fig. 2) shows the similarity in the river water and rainwater and the further similarity in proportions between these two kinds of water and seawater. The cations derived from the rocks of this basin, which also exemplifies a tropical river, are limited to Si and K.

Figure 3, which is based on the data of Fig. 1, is a diagrammatic representation of the mechanisms responsible for controlling the chemical compositions of the various bodies of water on

the surface of the earth. The precipitation control zone is one end-member of a series. The opposite end-member of this series is comprised of waters having as their dominant source of dissolved salts the rocks and soils of their basins. This grouping defines the second mechanism controlling world water chemistry as rock dominance. The waters of this rock-dominated end-member are more or less in partial equilibrium with the materials in their basins. Their positions within this grouping are dependent on the relief and climate of each basin and the composition of the material in each basin. It can be seen in Figs. 1 and 3 that the data for the large rivers of the world that drain tropical areas (the Congo, Orinoco, Niger) plot along the precipitation control-rock control series. Because 85 percent of the dissolved salts of the Amazon River are derived from the Andes, where the

rock contribution dominates as the controlling factor of the chemistry of the river (5), the data for this river, often thought of as a typical tropical river, plot geochemically nearer the rock-dominated end-member, although my data (5) show that many of the Amazon's tributaries—including the larger ones, such as the Rio Negro, which has an annual discharge three times that of the Mississippi River (5)—are prime examples of precipitation-dominated chemistry.

The third major mechanism that controls the chemical composition of the earth's surface waters is the evaporation-fractional crystallization process. As seen in Fig. 3, this mechanism produces a series extending from the Ca-rich, medium-salinity (freshwater), "rock source" end-member grouping to the opposite, Na-rich, high-salinity end-member. The rivers and lakes in this

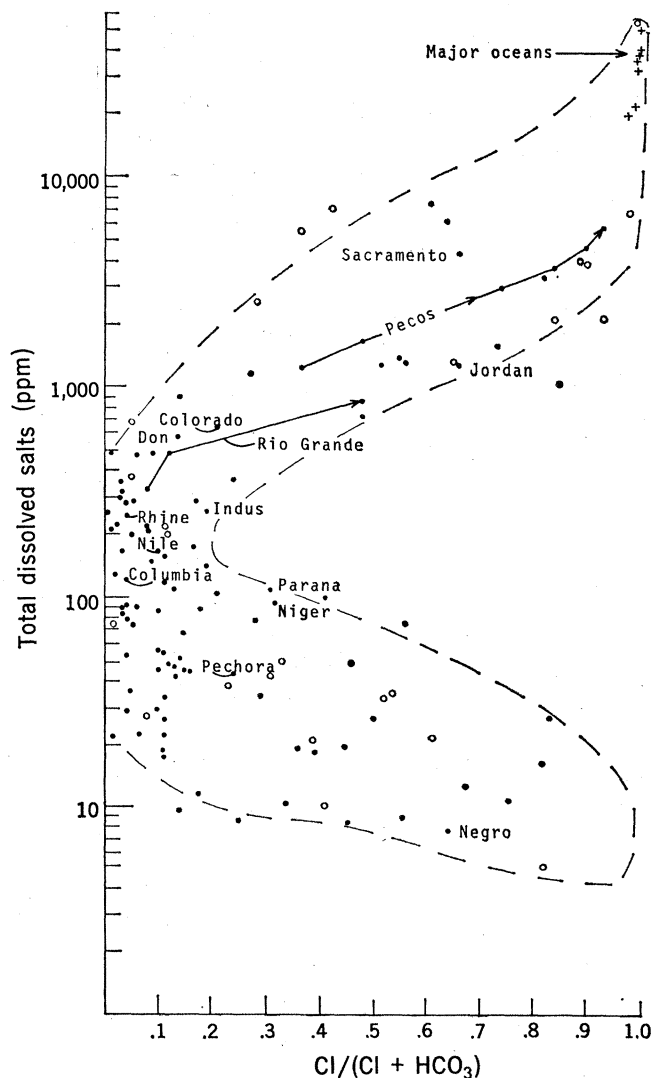
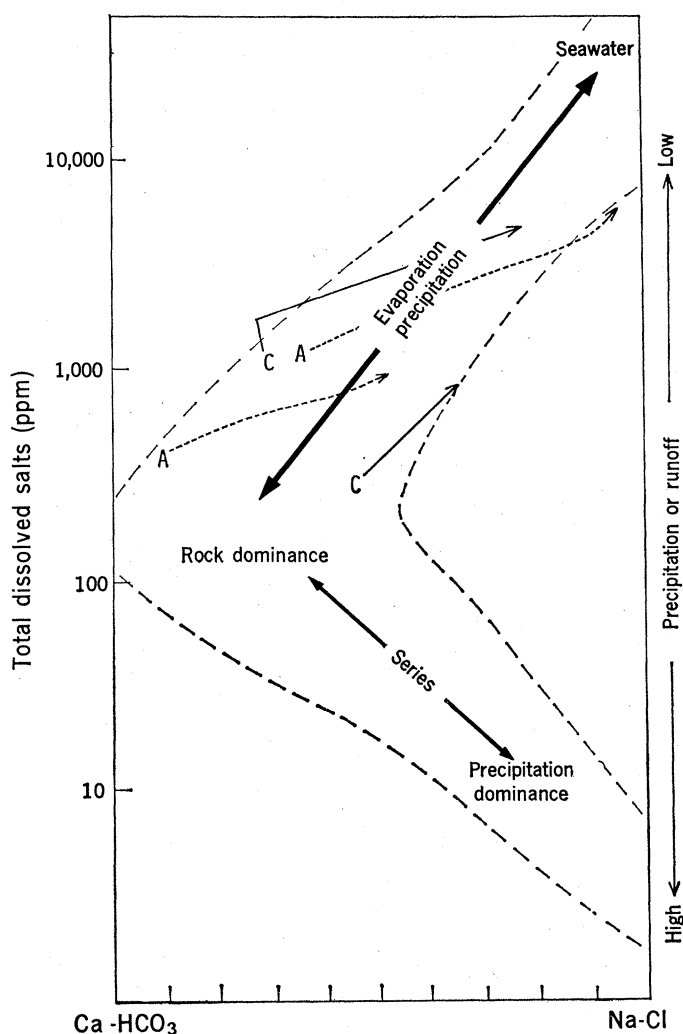


Fig. 3 (left). Diagrammatic representation of processes controlling the chemistry of world surface waters. Fig. 4 (right). Variation of  $\text{Cl}/(\text{Cl} + \text{HCO}_3)$  as a function of the total dissolved salts of world surface waters. ●, Rivers; ○, lakes; +, oceans.

Table 1. Source of Na, K, Mg, and Ca in various types of rivers.

River	Contribution from precipitation (%)	Contribution from rocks (%)
<i>Rain-dominated river type</i>		
Rio Tefé	81	19
<i>Rock-dominated river type</i>		
Ucayali	4.8	95.2
<i>Evaporation-crystallization river type</i>		
Rio Grande	0.1	99.9

group are usually located in hot, arid regions. A number of these rivers (the Pecos and the Rio Grande are good examples) show evolutionary paths, designated by arrows in Figs. 1 and 3, starting near the Ca or "rock source" end-member with changes in composition toward the Na-rich, high-salinity end-member as the rivers flow toward the ocean. This change in composition and concentration along the length of these rivers is due to evaporation, which increases salinity, and to precipitation of  $\text{CaCO}_3$  from solution, which increases the relative proportion of Na to Ca both from the tributaries and in the mainstream.

The Na-rich, high-salinity, end-member components are the various seawaters of the earth whose compositions (Fig. 1) cluster near the Na-rich axis. Seawater, however, cannot evolve simply from the concentration of freshwater and the precipitation of  $\text{CaCO}_3$ . Rather, as suggested by several researchers (1, 3, 4), there are other minor mechanisms—evaporation and crystallization—that contribute to the final exact composition of seawater.

Mass balance calculations of the contributions of Na, K, Mg, and Ca into three rivers exemplifying the three types of rivers described are given in Table 1. For each of the three river basins, the amount of dissolved salts contributed by precipitation was calculated from the sum of the concentrations of Ca, Na, K, and Mg multiplied by the annual precipitation. The calculations for precipitation contributions are based on data from chemical analysis of rain (5, 7) and yearly precipitation data (5, 8). The contributions from the rocks of the basins are logically assumed as the difference between river outflow and precipitation contribution. These calculations illustrate the precipitation dominance in the supply by precipitation of 81 percent of the Na, K,

Mg, and Ca carried by the Rio Tefé, an example of the rain-dominated type of river. The Rio Tefé is an Amazon tributary located 1700 km inland from the Atlantic.

The idea that these three major mechanisms—atmospheric precipitation, rock dominance, and the evaporation-crystallization process—control world water chemistry is borne out by a consideration of the major anions of the world's waters: chloride and bicarbonate. A presentation similar to that for the major cations (Fig. 1) is given in Fig. 4 for the major anions and total salinity. This presentation shows trends remarkably similar to those for cations and indicates support for the controlling mechanisms presented. For rivers in arid regions the evolutionary paths from the  $\text{HCO}_3$  end-member to the Cl end-member are again demonstrated by the data for the anions of the Rio Pecos and Rio Grande, plotted as arrows in Fig. 4.

For the axes showing data for total dissolved salts (Figs. 1, 3, and 4), precipitation or runoff data could be substituted without materially altering the interpretation. The great majority of Na-rich rivers and lakes of the world—both the humid and arid groupings of

Figs. 1 and 3—are in warm to hot climates.

In conclusion, these three mechanisms—atmospheric precipitation, rock dominance, and the evaporation-crystallization process—are the major factors controlling the composition of the dissolved salts of the world's waters. Other second-order factors, such as relief, vegetation, and composition of material in the basin dictate only minor deviations within the zones dominated by the three prime factors.

RONALD J. GIBBS

Department of Geological Sciences,  
Northwestern University,  
Evanston, Illinois 60201

#### References and Notes

1. E. J. Conway, *Proc. Roy. Irish Acad. Sect. B* **48**, 119 (1942).
2. E. Gorham, *Geol. Soc. Amer. Bull.* **72**, 795 (1961).
3. F. T. Mackenzie and R. Garrels, *Science* **150**, 57 (1965); *Amer. J. Sci.* **264**, 507 (1966).
4. L. G. Sillén, *Science* **156**, 1189 (1967).
5. R. J. Gibbs, in preparation.
6. D. A. Livingstone, *U.S. Geol. Surv. Prof. Pap.* **440-G** (1963), pp. 1-63.
7. J. H. Feth, *U.S. Geol. Surv. Prof. Pap.* **575-C** (1967), p. 223.
8. H. Bayer, Ed., *World Geographic Atlas* (Container Corporation of America, Chicago, 1953), p. 70.
9. E. D. Goldberg, in *Chemical Oceanography*, J. P. Riley and G. Skirrow, Eds. (Academic Press, London, 1965), p. 712.
10. Supported by the Office of Naval Research.

14 August 1970

## Radar Interferometric Observations of Venus at 70-Centimeter Wavelength

**Abstract.** A radar interferometer was used to map unambiguously the surface reflectivity of Venus in the polarized mode at a wavelength of 70 centimeters. The observed region extended from  $260^\circ$  to  $30^\circ$  in longitude and from  $-60^\circ$  to  $50^\circ$  in latitude with a surface resolution of approximately  $3^\circ$  by  $3^\circ$ . The result agrees well in most respects with earlier maps made elsewhere at shorter wavelengths and, in addition, discloses a number of new "features."

When delay-Doppler alone is used for discrimination, the mapping of scattering characteristics of planetary surfaces by Earth-based radar yields an ambiguity in the sign of one coordinate. An interferometer was first used by Rogers *et al.* (1) at Haystack Observatory in 1967 to resolve this ambiguity in Venus echoes at a wavelength of 3.8 cm. At the time of the 1969 inferior conjunction of Venus, greater sensitivity in their radar system enabled Rogers and Ingalls (2, 3) to improve the earlier map of surface scattering.

In this report we describe interferometer observations of Venus made at the Arecibo Observatory in 1969 at a substantially longer wavelength (70 cm)

than was used at Haystack and with coverage of a somewhat larger area of the surface. It was hoped that a comparison between maps at such different wavelengths might yield an indication of the scale sizes of the planetary surface irregularities that are primarily responsible for the backscattered power at large angles of incidence. The Arecibo interferometer that was used to receive the echoes consisted of the basic 1000-foot (300-m) reflector (which was also used as the transmitting antenna) and a fixed parabolic reflector of 100-foot (30-m) diameter, with a movable offset feed that allowed tracking up to  $10^\circ$  from the zenith. The parabola was located 10.8 km to the north-